JOURNAL OF GEOPHYSICAL RESEARCH, VOL. 113, D22110, doi:10.1029/2008JD010000, 2008

Comparison of upper tropospheric water vapor observations from the Microwave Limb Sounder and Atmospheric Infrared Sounder

Eric J. Fetzer,[1] William G. Read,[1] Duane Waliser,[1] Brian H. Kahn,[1] Baijun Tian,[1,2] Holger Vömel,[3] Fredrick W. Irion,[1] Hui Su,[1] Annmarie Eldering,[1] Manuel de la Torre Juarez,[1] Jonathan Jiang,[1] and Van Dang[1]

Received 20 February 2008; revised 2 September 2008; accepted 23 September 2008; published 29 November 2008.

[1] We compare matched retrievals of upper tropospheric water vapor (UTWV) mixing ratios from the Microwave Limb Sounder (MLS) instrument on the Aura satellite, and the Atmospheric Infrared Sounder (AIRS) instrument on the Aqua satellite. Because each instrument's sampling is affected by tropical conditions, about half of mutually observed scenes in the tropics yield simultaneous successful retrievals from both systems. The fraction of mutually retrieved scenes drops to 30% at higher latitudes where clouds significantly inhibit AIRS sounding. Essentially all scenes observed by MLS in extratropical and polar regions yield successful retrievals. At 250 hPa in the tropics, measurements from the two instruments are highly correlated, the differences of their means ($\bar{\Delta}_q$) are smaller than 10%, and the standard deviations of their differences (σ_q) are 30% or less. At 300 hPa, MLS means are drier by 10–15%, and σ_q is 40–60%, indicating that responses of MLS and AIRS to UTWV perturbations are not one-to-one. Root mean square agreement is also poorer over the poles at 300 hPa and at 200 and 150 hPa at lower latitudes. In these regions, $|\bar{\Delta}_q|$ = 10% or more, and σ_q = 40–70%. Correlations between the two data sets are 0.7–0.9 at 300 and 250 hPa globally and at 200 hPa in the tropics. This high correlation indicates that σ_q of 50% or greater comes mainly from systematic differences in sensitivity of the two instruments, especially for small and large UTWV amounts; larger values of σ_q are generally not due to large random errors from either instrument. An AIRS low-end sensitivity threshold of 15–20 ppmv leads to poorer agreement under the driest conditions. Disagreement at 300 hPa likely comes from overestimation by MLS for the wettest conditions of >400 ppmv. While MLS is biased slightly dry overall at 300 hPa, it is biased wet in the wettest regions, particularly those associated with deep convection. These sensitivity differences explain nonunity slopes of linear fits to the two data sets. MLS everywhere has a greater dynamic range than AIRS, with larger maxima and smaller minima. Good agreement at 250 hPa suggests AIRS uncertainties of 25% up to the reported 250–200 hPa layer in the tropics and extratropics, consistent with previous comparisons with balloon- and aircraft-borne instruments. The agreement at 250 hPa also indicates that MLS is reliable from its reported 215-hPa level upward in altitude.

Citation: Fetzer, E. J., et al. (2008), Comparison of upper tropospheric water vapor observations from the Microwave Limb Sounder and Atmospheric Infrared Sounder, *J. Geophys. Res.*, *113*, D22110, doi:10.1029/2008JD010000.

1. Introduction

[2] Improved global observations of upper tropospheric water vapor (UTWV) are critical in answering several unresolved climate questions. UTWV is particularly important in climate feedback mechanisms, either directly through radiative effects, or indirectly through cloud formation processes. The size of these feedbacks is still in question [*Held and Soden*, 2000; *Stephens*, 2005; *Bony et al.*, 2006; *Soden and Held*, 2006]. UTWV is significant in determining the atmospheric radiative balance, especially in partially cloudy and cloud-free scenes [*L'Ecuyer and Stephens*, 2003; *Lin et al.*, 2006]. The relationship between UTWV and cloud formation processes is an active area of research [*Jensen et al.*, 2000; *Eguchi and Shiotani*, 2004; *Liu*, 2007; *Peter et al.*, 2006]. Any possible indirect effects of aerosol on radiative and precipitative properties of cirrus clouds are mediated by UTWV [*Kärcher and Lohmann*, 2003; *Jensen and Ackerman*, 2006; *Massie et al.*, 2007]. Also, UTWV

[1] Jet Propulsion Laboratory, California Institute of Technology, Pasadena, California, USA.
[2] Joint Institute for Regional Earth System Science and Engineering, University of California, Los Angeles, California, USA.
[3] Deutscher Wetterdienst, Lindenberg, Germany.

0148-0227/08/2008JD010000$09.00

and upper tropospheric temperature are important factors in stratospheric hydration mechanisms [*Holton et al.*, 1995; *Sherwood and Dessler*, 2001; *Holton and Gettelman*, 2001; *Liu et al.*, 2007].

[3] We compare height-resolved water vapor mixing ratios from two independent satellite observing systems at pressures from 300 to 150 hPa. The Atmospheric Infrared Sounder (AIRS) experiment, in operation since September 2002 on the Aqua spacecraft, utilizes a combination of infrared and microwave radiances observed near nadir to retrieve mixing ratios from the surface to the upper troposphere [*Aumann et al.*, 2003]. The Earth Observing System Microwave Limb Sounder (EOS MLS; hereafter referred to as MLS), operating since July 2004 on the Aura spacecraft, observes microwave emissions from the limb. MLS radiances are inverted to profiles of mixing ratio from 316 hPa into the mesosphere [*Waters et al.*, 2006]. Both MLS and AIRS retrieve temperature, minor gases, and cloud properties along with water vapor mixing ratios. Although MLS and AIRS are carried on separate satellites, they fly in close formation in the NASA A-Train satellite constellation, so the two systems' observations are co-located and separated in time by about 8 minutes [*Stephens et al.*, 2002]. Because MLS and AIRS use fundamentally different observing methods that are sensitive to different atmospheric conditions, a combination of observations from both instruments offers the potential of a more complete UTWV climatology than either instrument can provide individually. However, the two sets of observations must first be compared to characterize their relative uncertainties, and must be reconciled with correlative observations, typically from radiosondes and aircraft.

[4] AIRS and MLS comparisons shown here are limited to those mutually observed upper tropospheric scenes where both instruments return a valid retrieval. This approach is similar to comparisons between satellite and in situ data, which are typically also limited to those conditions where the satellite instrument can retrieve information. We do not compare AIRS and MLS in the stratosphere because AIRS reported stratospheric water vapor is, at best, able to reproduce the mean climatology of a region and period [*Gettelman et al.*, 2004; *Read et al.*, 2007].

[5] The potential effects of reduced sampling rates on both instruments are examined in Fetzer et al. [The effect of sampling on upper tropospheric water vapor climatologies from the Microwave Limb Sounder and Atmospheric Infrared Sounder, manuscript in preparation, 2008]. As will be shown below, the two instruments can simultaneously retrieve UTWV for roughly 40 to 70% of all observed scenes within a 15° latitude band; this study is concerned with those scenes. The remaining scenes are not observed by either AIRS or MLS primarily because clouds may affect upwelling radiation from UTWV. Sampling characteristics are relevant because AIRS sounding is prevented by thicker clouds, However, some observations are attained by AIRS for up to 70% effective cloud cover because the AIRS retrieval method exploits microwave information to partially remove the effects of clouds [*Susskind et al.*, 2006; *Fetzer et al.*, 2006]. MLS constituent sampling is partially affected by ice particles [*Livesey et al.*, 2006a, 2006b; *Wu et al.*, 2006], but MLS retrieval algorithms may also fail in regions where the a priori solution is unrepresentative [*Read et al.*, 2007]. Scattering by ice particles appears to be the dominant source of failed MLS retrievals in tropical regions with extensive cloud cover. (However, as discussed below, other factors can lead to failed MLS retrievals under clear tropical conditions.) Both instruments are capable of making some UTWV observations under cloudy conditions. An understanding of the effects of cloud on both instruments is a necessary step toward creating a complete and representative UTWV climatology. The goal of this study is a constraint on the relative uncertainties of the two instruments when they simultaneously observe.

[6] UTWV observations are available from other instruments besides AIRS and MLS. Balloon-based observations of UTWV are limited because operational radiosonde instruments are insensitive to water vapor for the cold, dry conditions typical of pressures less than about 300 hPa [*Ferrare et al.*, 2004; *Whiteman et al.*, 2006; *Miloshevich et al.*, 2006]. The sensitive balloon-borne instruments described in *Vömel et al.* [2007] are used to validate MLS water vapor under very dry stratospheric conditions. Aircraft observations are of high quality but limited extent [e. g., *Gettelman et al.*, 2004]. A variety of operational satellite instruments in both geostationary and low-earth orbits carry a 6.7 μm channel sensitive to water vapor. While operational satellite UTWV measurements are limited to relative humidity over a layer several kilometers thick [*Soden and Bretherton*, 1993], their coverage extends nearly 30 years. In addition, operational sounders in geosynchronous orbit can be used to examine the diurnal cycle [*Soden*, 2000; *Tian et al.*, 2004]. (In contrast, AIRS and MLS can each retrieve temperature and absolute humidity over 1–3 km thick layers, but their coverage is limited to a few years. Also, because they are in sun-synchronous orbits they sample only two points in the diurnal cycle.) Other observations of upper tropospheric relative humidity from an earlier version of the Microwave Limb Sounder instrument on the Upper Atmospheric Research Satellite (*UARS*/MLS) launched in 1991 [*Read et al.*, 2001] have been used to study water vapor feedback processes [*Minschwaner and Dessler*, 2004].

[7] The structure of this paper is as follows. Section 2 describes the AIRS and MLS observing methodologies, the viewing geometries of the two systems, the instruments' coverage, and the validation state of both data sources. (An Appendix describes the quality flagging and the procedure for matching the two data sets.) Section 3 presents time-zonal mean statistics of the fraction of converged retrievals, mean UTWV, mean UTWV differences, standard deviation of differences, sampling extrema of matched data, correlations, and degree of linearity of the two data sets (as measured by slopes of fitted lines). Section 3 also interprets the performance of the separate instruments by season, pressure and latitude. Section 4 presents a summary of the conclusions about instrument performance reached in section 3. Section 4 also discusses the implications of this work for other studies, and suggests further research.

2. Data Sources

[8] This section describes basic characteristics of the AIRS and MLS instruments, their validation status, their

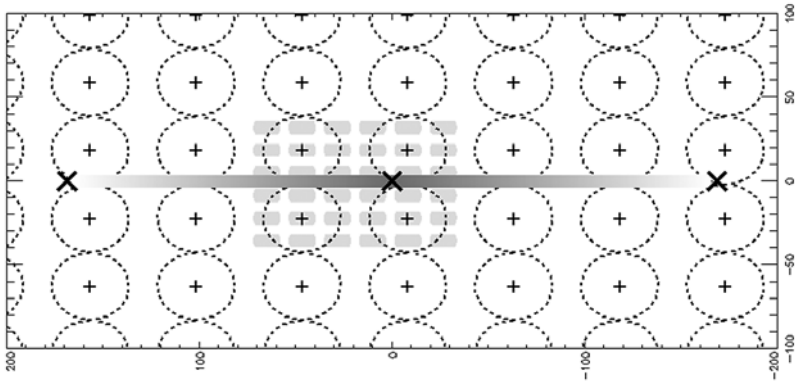

Figure 1. Plan view of MLS and AIRS/AMSU viewing geometries with MLS tangent points as bold cross, central MLS averaging kernel as a broad gray line, and approximate AMSU response functions as dashed ovals with pluses at their center. Nine AIRS spatial response functions are represented as shaded oblongs for each of four AMSU fields of view nearest the MLS tangent point.

viewing geometries, and the importance of excluding AIRS stratospheric water vapor values. The Appendix provides addition discussions of quality flags and the data matching method used in this study.

2.1. Atmospheric Infrared Sounder

[9] The AIRS experiment was launched on the Aqua spacecraft on 4 May 2002, and became fully functional on 1 September 2002. Aqua is in a sun-synchronous orbit with an equator crossing time of 1:30 AM (PM) on the southward or descending (northward or ascending) orbit. Observations from Aqua are intended to improve our understanding of the Earth's hydrologic cycle [*Parkinson*, 2003]. The AIRS experiment includes the AIRS instrument [*Pagano et al.*, 2003] and two microwave sounding instruments: the Advanced Microwave Sounding Unit (AMSU) and the Humidity Sounder for Brazil (HSB) [*Lambrigtsen*, 2003]. HSB improves the water vapor retrieval capability of the AIRS system [*Fetzer et al.*, 2006], but ceased operating in February 2003, some eighteen months before the launch of MLS. All results presented here use AIRS/AMSU retrievals. A retrieval algorithm inverts observed radiances from AIRS and AMSU to vertical profiles of temperature, minor gases, and water vapor, along with cloud amount, cloud top properties, and surface properties [*Susskind et al.*, 2003, 2006]. The AIRS and AMSU instruments view downward, scanning in a swath about 1600 km wide, with a maximum viewing angle of 49.5° from nadir. The horizontal spacing of AIRS profile quantities is about 45 km at nadir, with thirty retrieved profiles across the viewing swath. (This is the AMSU resolution, while the AIRS instrument samples infrared spectra at three times higher horizontal resolution; see discussion of Figure 1 below.) Each profile is retrieved from a set of nine observed AIRS spectra and one observed AMSU spectrum. The AMSU observation rate is 324,000 spectra per day, so up to 324,000 profiles may be retrieved daily. Because clouds can block infrared radiances from below, roughly 30% of possible profiles are retrieved from the AMSU microwave observations alone [*Susskind et al.*, 2006]; that fraction varies considerably with location and the prevalence of clouds [*Fetzer et al.*, 2006]. Microwave-only retrievals are excluded from this study because they contain no UTWV information. Below we discuss instruments "yields." For AIRS this effectively means the percentage of retrievals where clouds do not significantly obscure the infrared radiances emitted from below those clouds. This study uses AIRS Version 4.0 Level data, available at http://airs.jpl.nasa.gov/.

[10] The AIRS system was designed and built to resolve water vapor with 15% root mean square (RMS) uncertainty in 2 km layers in the troposphere. AIRS UTWV in the tropics has been compared in several studies with in situ observations using data from aircraft [*Gettelman et al.*, 2004] and balloons [*Hagan et al.*, 2004; *Tobin et al.*, 2006], though at a limited set of locations. Other studies [*Divakarla et al.*, 2006; *Tobin et al.*, 2006; *Nalli et al.*, 2006; *Susskind et al.*, 2006; *Fetzer et al.*, 2004, 2006; *Ye et al.*, 2007] have compared AIRS total precipitable water, lower tropospheric water vapor, and temperature profiles with observations from a variety of correlative data sources regionally and globally. In summary, these studies show individual AIRS specific humidity profiles have RMS measurement uncertainties of ±10–30%, and measurement biases of 10% or less in 2 km layers in nonpolar regions. As noted by *Hearty et al.* [2007], the AIRS Version 5.0 data have smaller UTWV bias relative to radiosondes than earlier data releases, including the V4.0 data discussed here. The RMS characteristics of AIRS Version 4.0 and Version 5.0 data are very similar [*Hearty et al.*, 2007].

[11] As discussed by *Read et al.* [2007], vertical resolution estimates are based on the retrieval averaging kernels. Because the AIRS Version 4.0 data used in this study do not provide averaging kernels, we presume that the AIRS resolution is near 2 km, as determined through simulation by *Susskind et al.* [2003]. Averaging kernels are being provided as part of Version 5.0 data, first available in the summer of 2007. Preliminary comparisons of the AIRS V5.0 data with in situ observations corroborate the V4.0 results. *Maddy and Barnet* [2008] examine AIRS vertical resolution in Version 5.0 data, and report water vapor resolution of 2–3 km throughout the troposphere.

2.2. Aura Microwave Limb Sounder

[12] MLS is a limb-scanning microwave radiometer on the Aura spacecraft, launched on 14 July 2006. Aura and

Table 1. Definition of Symbols for Quantities Discussed in Section 3

Quantity	Definition
$\bar{q}$	Mean MLS and AIRS UTWV in ppmv
$\bar{\Delta}_q$	Bias between mean matched AIRS and MLS (AIRS minus MLS) UTWV, as percentage of $\bar{q}$
σ_q	Standard deviation of the difference of matched AIRS and MLS UTWV observations as percentage of $\bar{q}$
$q_{MLS-3\%}$	The third percentile (driest 3%) of MLS observed UTWV in ppmv
$\%_{AIRS-3\%}$	The third percentile (driest 3%) of AIRS observations as percentage of $q_{MLS-3\%}$
$q_{MLS-97\%}$	The 97th percentile (wettest 97%) of MLS observations in ppmv
$\%_{AIRS-97\%}$	The 97th percentile of AIRS observations (wettest 97%) as a percentage of $q_{MLS-97\%}$
ρ	The linear correlation coefficient between AIRS and MLS UTWV
m	The slope of the least squares fitted line of AIRS to MLS

Aqua (carrying AIRS) fly in the A-Train formation, with Aqua leading by 15 minutes. Observations from instruments on Aura are intended to answer a number of important questions about atmospheric processes, with a particular emphasis on chemical constituents [*Schoeberl et al.*, 2006]. Observed microwave radiances from MLS are inverted to profiles of temperature, geopotential height, cloud ice, and several minor gases, including water vapor from the upper troposphere into the stratosphere [*Waters et al.*, 2006]. MLS points in a fixed azimuth and its data are sampled along a single track slightly displaced from the orbit track. Because MLS views in the forward direction, AIRS and MLS observations are spaced in time by roughly eight minutes despite a spacecraft separation time of fifteen minutes. MLS retrievals are spaced horizontally by 165 km [*Livesey et al.*, 2006b]. The maximum MLS global retrieval rate is 3494 profiles per day. This study uses Version 1.5 water vapor retrievals publicly available at the Goddard Spaceflight Center DAAC through http://mls.jpl.nasa.gov.

[13] The rate of successful MLS retrievals is much higher than for AIRS, though it can be as low as 50% in the moist tropics. The causes of unsuccessful MLS yields are two-fold. Roughly two-thirds of MLS tropical retrievals are unsuccessful due to non-representative a priori solutions [*Read et al.*, 2007]. This occurs most commonly under clear but moist conditions. The remaining third of unsuccessful MLS retrievals is a consequence of upwelling microwave radiances from water vapor being scattered from larger ice particles, of diameters greater than 200 μm [*Wu et al.*, 2005, 2006]. This scattering distorts the line shapes so that spectral fits cannot be obtained in the retrieval. Of course, these unsuccessful retrievals are most common in cloudiest conditions.

[14] *Froidevaux et al.* [2006] report a preliminary RMS uncertainty estimate for MLS Version 1.5 UTWV of 17% or less. This estimate is based on an error model internal to the MLS retrieval system. That study also includes a comparison of AIRS and MLS UTWV. Froidevaux et al. did not discriminate between stratospheric conditions, as is done here, or eliminate UTWV values of less than 20 ppmv, as was done by *Read et al.* [2007]. *Froidevaux et al.* [2006] report bias of AIRS relative to MLS of −12 to +25% and standard deviations of their differences of ±53 to ±125%, with percentages relative to the mean UTWV. (These numbers are analogous to $\bar{\Delta}_q$ and σ_q, as defined in Table 1). In contrast, *Read et al.* [2007] and this study both show AIRS-MLS UTWV RMS agreement is as good as ±30% (analogous to the RMS of $\bar{\Delta}_q$ and σ_q). The improvement in agreement is primarily a consequence of the exclusion of stratospheric observations. More recently, *Vömel et al.* [2007] compared MLS UTWV against very accurate Cryogenic Frostpoint Hygrometer (CFH) instruments on balloons, and report MLS Version 1.5 dry biases of about 25% near 300 hPa, with smaller biases at lower pressures. The standard deviations of the differences are 25–40%. *Vömel et al.* [2007] show CFH-MLS agreement improves for drier, colder conditions, with best agreement for the very low mixing ratios of a few ppmv typical of the stratosphere. *Read et al.* [2007] show that both MLS Version 1.5 and 2.2 data at 316 hPa have an overall dry bias of ∼25% relative to AIRS, but a wet bias for wettest scenes at 300 hPa when mixing ratios are 500 to 1000 ppmv. MLS again becomes drier above about 1000 ppmv, but these wettest values are very infrequent. *Read et al.* [2007] ascribe the MLS wet bias in wet scenes to an error of ∼1% in transmissivity in the MLS forward radiative transfer model. So, at 316 hPa MLS is biased dry in the mean, but is biased wet for scenes greater than 500 ppmv. Read et al. also find in comparison with MLS that AIRS loses sensitivity around 20 ppmv, broadly consistent with *Gettelman et al.* [2004] who suggested a 15 ppmv threshold for AIRS. Read et al. note that MLS has a lower sensitivity threshold of 3–4 ppmv, well below typical UTWV values discussed here.

2.3. Viewing Geometries and Coverage

[15] Figure 1 shows the local viewing geometries of MLS and AIRS. Most of the MLS signal is received from a roughly 3 km vertical by 7 km cross-track by 180 km along-track volume along the tangent path [*Livesey et al.*, 2006b]. The MLS horizontal averaging kernel is shaded in Figure 1; this represents the weighted contribution to the signal by the UTWV field. In contrast, most of the AMSU- and AIRS-observed radiance is emitted from a single AMSU field of view represented by dashed circles in Figure 1, and the nine corresponding AIRS infrared radiance observing fields of view shown as shaded oblongs. The infrared radiances provide most of the information for the AIRS UTWV retrievals, with the AMSU microwave observations primarily constraining the AIRS total water vapor. The vertical resolution of MLS is due mainly to the vertically confined viewing geometry as discussed by *Livesey et al.* [2006b]. The AIRS vertical resolution comes from the large number of water vapor, carbon dioxide and other constituent spectral lines in the AIRS spectra [*Strow et al.*, 2006]. The AIRS retrieval algorithm essentially deconvolves the many weighting functions to resolve vertical scales smaller than an individual weighting function's thickness. Figure 1 also suggests the density of sampling by the two instruments. Figure 9 of *Read et al.* [2007] shows the regional coverage of AIRS and MLS, and clearly illustrates the roughly 100-fold greater coverage by AIRS.

2.4. Exclusion of AIRS Stratospheric Values

[16] In addition to the quality flag screening discussed in the Appendix, care must be taken to include only those

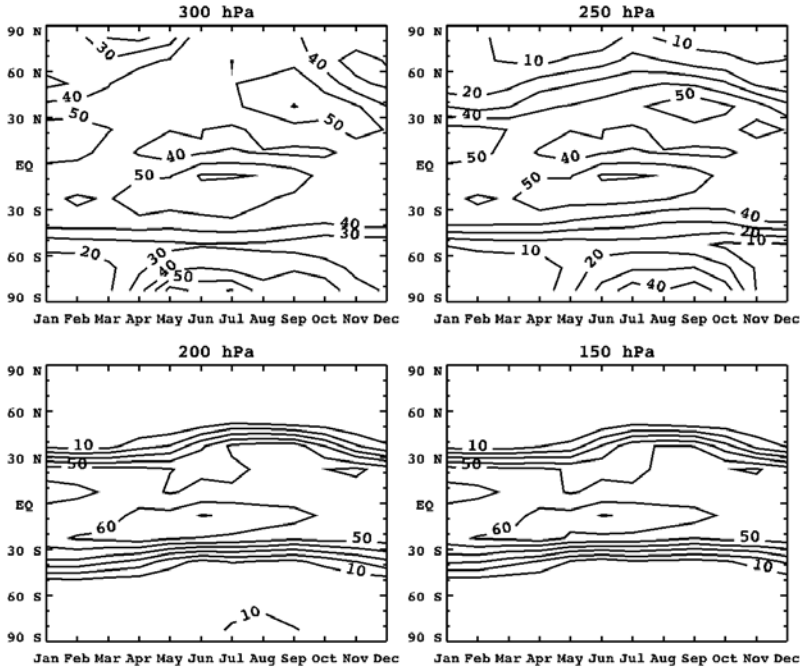

Figure 2. Fraction of matched AIRS-MLS retrieval pairs where both systems provide successful retrievals, as percent of all MLS soundings, in twelve 15-degree latitude bands and 12 months in 2005.

portions of AIRS UTWV profiles within the troposphere. The AIRS system is sensitive only to tropospheric water vapor amounts [*Susskind et al.*, 2003]. This rejection of stratospheric values is especially important in polar regions, where tropopause pressures can be 300 hPa or greater. AIRS lower stratospheric water vapor values may be misleading because their means and those from MLS may differ by only a few percent, while the correlation between AIRS and MLS stratospheric water vapor is zero to high statistical significance.

[17] Because AIRS has only climate-mean skill (at best) in the stratosphere, this study considers only those portions of AIRS UTWV profiles where pressures are greater than the WMO-defined AIRS retrieved tropopause pressure [*World Meteorological Organization*, 1957]. Tropopause pressure is derived from the AIRS temperature-pressure profile, and reported in the AIRS data files. It is reported to a few hundred meters, finer than the 1–3 km resolution of the AIRS temperature and humidity profiles. Preliminary comparisons of AIRS and Global Positioning System retrieved temperature profiles show tropopause log-pressure altitude agreement to within about ±0.5 km globally for January 2003.

3. Comparison of Matched Observations

[18] In this section we present zonal mean summaries of all matched AIRS-MLS retrieval pairs of highest quality from both instruments. Summaries are shown for each of the twelve months in 2005, and in twelve zonal bands between the poles, defined as [90–75S, 75–60S, ..., 75–90N]. While the poles are given as the limits of the comparison, note that viewing geometry restricts the extreme MLS latitudes (and so the latitudes of highest matched AIRS-MLS observations) to ±81.8°. For this study we examined a number of quantities pertinent to the individual instruments' measurements, and their matched differences. These include statistical moments (means and variances), ranked statistics (medians and quantiles), and correlation coefficients (both Pearson and nonparametric estimators). The results of those comparisons are presented here primarily as means, biases, standard deviations, extrema, Pearson correlation coefficients, and the slopes of fitted lines. We show these quantities because instrument performance is generally specified in terms of the measurement bias (accuracy) and standard deviation (precision), or the root mean square of the two [*Aumann et al.*, 2003]. As will be seen, root mean square (RMS) differences may be large even when the two data sets are highly correlated, suggesting both instruments are sensitive to a wide range of UTWV conditions, but have different responses to those conditions.

3.1. Retrieval Sampling Rates

[19] Figure 2 shows combined AIRS and MLS yields. Yield is defined here as the percentage of all possible pairs of matched MLS-AIRS soundings containing successful UTWV retrievals from both instruments. (The number of possible pairs is also the total number of MLS soundings. The numbers shown here are presumed to be representative of the roughly hundred-fold denser AIRS coverage.) An individual instrument's yield is defined here as the fraction of matched pairs where that instrument has highest-quality retrievals, irrespective of the other instrument's retrieval status. The total number of matched pairs in a monthly-15 degree latitude zonal bin is typically four to seven thousand, so yields of even 10% represent samples of several hundred. This implies that all the quantities shown are statistically significant to a high level of confidence.

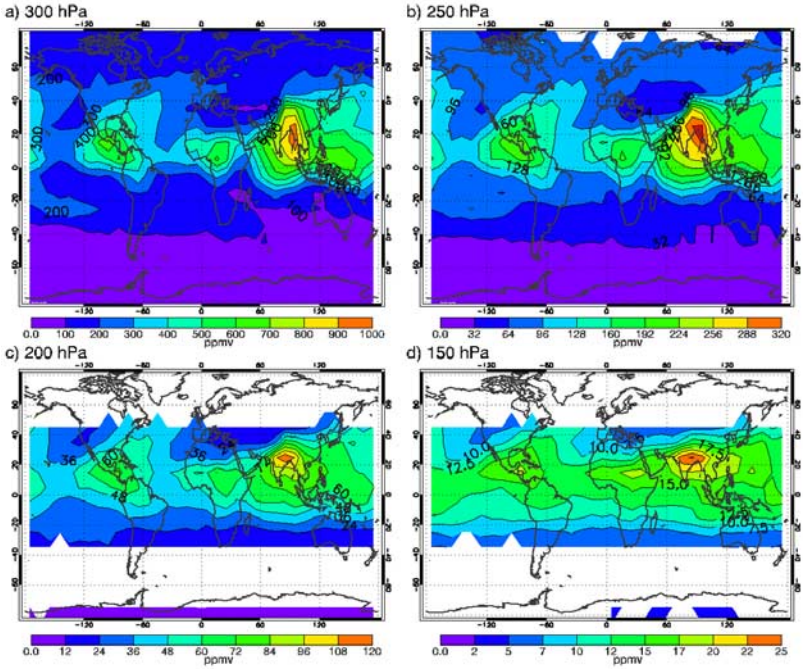

Figure 3. Mean UTWV maps from combined matched AIRS and MLS observations for July–September 2005. Blank regions represent regions where fewer than 10% of samples are within the AIRS-defined troposphere.

[20] Several factors determine the distribution of yields in Figure 2, and the most dramatic is the effect of a lower tropopause at high latitudes. This explains why the 10% contour is often equatorward of ±50° latitude at 150 hPa. Other high-latitude reductions in yields at 300 and 250 hPa in Figure 2 are almost entirely a consequence of decreased AIRS yields because of extensive high-latitude cloudiness. See the study of *Fetzer et al.* [2006] for a discussion of the effects of cloud type on AIRS water vapor sampling. Roughly 35 to 50% of all AIRS retrievals pass highest quality control at high latitudes, with an AIRS-only yield local maximum at 300 hPa of about 65% over the Antarctic Plateau during austral winter, presumably due to very clear conditions there. (Lower pressures have larger numbers of stratospheric cases even when the retrievals are successful.) Also, the lowest AIRS yields of 20–30% in Figure 2 are found in the 45–60 S band, consistent with the very cloudy conditions prevalent over the Southern Ocean. The MLS yields at all pressures of interest here are nearly 100% for latitudes poleward of 45°.

[21] At latitudes between 45 S and 45 N the yields in Figure 2 are explained by reductions in sampling by both AIRS and MLS. This is most apparent in the tropics, where minimum zonal mean yields of 40–50% are seen in the summer hemisphere. This summertime minimum is likely due to deep convective clouds reducing the sounding capability of both instruments.

[22] The largest low-latitude yields in Figure 2 are found in the wintertime subtropical belts, presumably associated with diminished high level cloud cover [*Rossow and Schiffer*, 1999]. *Fetzer et al.* [2006] showed maxima in AIRS yields as large as 90% in the wintertime subtropics near the centers of the ocean basins. Here the MLS yields are comparable to AIRS. However, the zonal means shown in Figure 2 include opaque cloudiness associated with baroclinic wave activity in the winter equatorial hemisphere in all months, reducing yields to the 60–70% values shown. Compared to high latitudes, the effect of lower tropopause altitude is relatively minor in the tropics and subtropics, and contributes 20–40% of the reduced yield at 200 and 150 hPa from ±30–45° latitude during winter.

3.2. Mean Maps and Sampling Distributions of Matched Observations

[23] Figure 3 shows maps of the mean MLS and AIRS UTWV during July–September 2005. Here mean water vapor is defined to be $\bar{q} = (\bar{q}_{MLS} + \bar{q}_{AIRS})/2$. (See Table 1 for definitions of all symbols used in this and the following discussions.) Yields of less than 10% are represented as missing data in Figure 3 (and subsequent figures), indicating prevalent stratospheric conditions. This illustrates how the 200 hPa surface is usually in the stratosphere at middle and high latitudes. Several other features are apparent from Figure 3, including a global maximum over the Asian Monsoon region at all levels [*Fu et al.*, 2006], local maxima over the continents (presumably associated with transport to the upper troposphere by enhanced convective uplift), and decreasing UTWV moving both poleward and to lower pressures. In addition to a 10- to 30-fold decrease between 300 and 150 hPa, the water vapor fields in Figure 3 become more zonally symmetric moving upward. This is presumably associated with more vigorous convection over the continents causing more frequent convective penetration to 100–150 hPa [*Betts*, 1973; *Yanai et al.*, 1973; *Highwood and Hoskins*, 1998; *Hartmann and Larson*, 2003; *Folkins and Martin*, 2005]. At 300 and 250 hPa in Figure 3 the southern winter polar regions are roughly half as moist as the northern polar regions, consistent with significantly

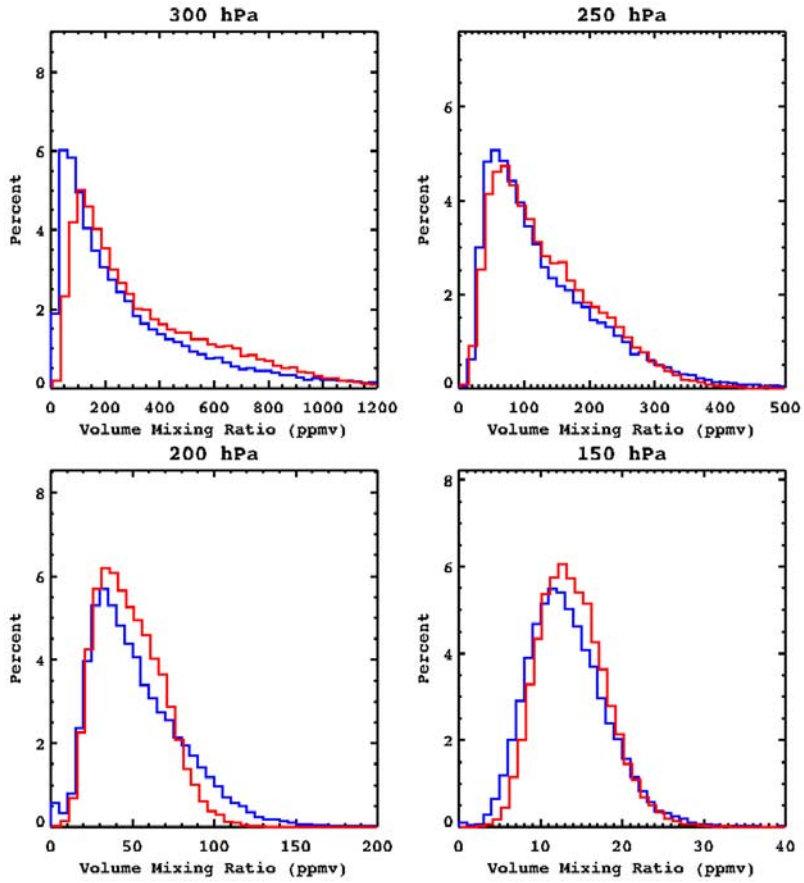

Figure 4. Distribution of UTWV from matched MLS (blue histograms) and AIRS (red histograms) retrievals for the latitude range ±15 degrees and the period July–September 2005. Bin size is 30 ppmv at 300 hPa, 12.5 ppmv at 250 hPa, 5 ppmv at 200 hPa, and 1 ppmv at 150 hPa.

lower temperatures in the upper troposphere in the winter hemisphere. The poleward and upward decreases in water vapor have implications for AIRS sensitivity. Note that the mean 250 hPa water vapor is below 32 ppmv southward of about 40 S. This suggests that scenes drier than the nominal 15–20 ppmv lower sensitivity limit of AIRS [*Gettelman et al.*, 2004; *Read et al.*, 2007] are common there. Similarly, the 150 hPa water vapor is primarily 20 ppmv or drier, suggesting AIRS is insensitive to prevalent conditions at 150 hPa. However, AIRS may be quite capable of sensing the very wettest conditions locally over Asia at 150 hPa during northern summer, as well as near and within thin cirrus clouds surrounding convection throughout the tropics [*Kahn et al.*, 2008]. MLS may be less sensitive to the very wettest conditions at 300 hPa in Figure 3, especially over the convective regions where mean water vapor is 400 ppmv or greater, and the MLS water vapor signal may reach saturation.

[24] Figure 4 shows histograms of UTWV from MLS and AIRS in the 15 S to 15 N latitude band during July to September 2005. These plots show the same data used to create the tropical portion of the maps shown in Figure 3. Because the histograms in Figure 4 are generated from matched retrievals, differences between the curves in Figure 4 indicate different responses to UTWV from AIRS and MLS. At 300 hPa MLS observes more of the driest scenes. The cause of the MLS 300 hPa dry bias noted by *Read et al.* [2007] is apparent from Figure 4: the MLS PDF is skewed toward drier values, with a peak shifted ~60 ppmv lower than AIRS. Note that the 300 hPa bin size is 30 ppmv, so the difference at 300 hPa for all but the smallest bin cannot be attributed to AIRS insensitivity to low UTWV. At 250 hPa the agreement between the two curves is clearly better than at any other pressure level. As will be seen, AIRS and MLS UTWV have very similar characteristics at 250 hPa. The histograms are again noticeably different at 200 hPa, with quite good agreement for driest scenes, but with the AIRS curve now more sharply peaked. By 150 hPa, the distributions from both instruments are of similar shape, but with AIRS showing a slight moist bias. (We presume AIRS is biased because roughly half the samples at 150 hPa are obtained for scenes less with than 15–20 ppmv of water vapor, the nominal lower limit of sensitivity for AIRS.)

3.3. Zonal Means, Biases, and Standard Deviations of Differences of Matched Observations

[25] Figure 5 shows mean time-zonal UTWV ($\bar{q}$), defined as averages of the MLS and AIRS means, for the twelve months, twelve zonal bands, and four pressures of interest. Note that these means are not the average of all observations from AIRS and MLS, but are instead limited to the fraction of matched pairs whose yields are shown in Figure 2. Here we define $\bar{q}$ to be the arithmetic mean of the AIRS and MLS means (their sum divided by two). The limited number of

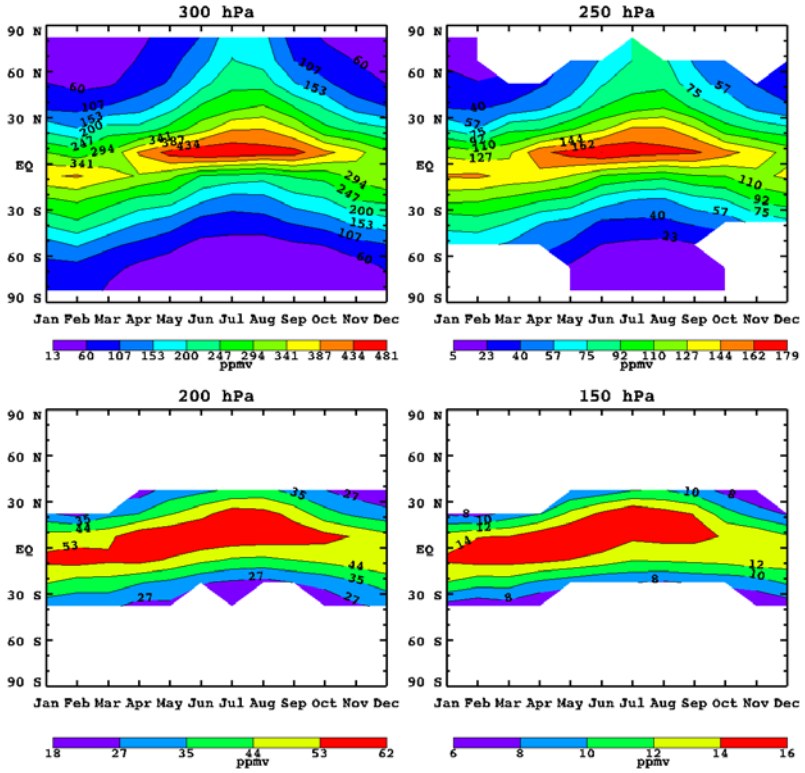

Figure 5. Time-zonal means of the average AIRS and MLS water vapor mixing ratios from matched MLS and AIRS retrieval pairs ($\bar{q}$) by latitude and month in 2005.

any tropospheric observations at 200 and 150 hPa poleward of about 50° latitude in Figure 5 follows from the very low yields seen there in Figure 2. Note that the largest $\bar{q}$ is found in the 0–15 N band at 300 hPa between May and August. This maximum extends upward to all other levels. Drier regions are encountered when moving upward and poleward from the tropics at 300 hPa, including a roughly thirty-fold decrease in mean mixing ratios between 300 and 150 hPa, and an eight-fold decrease between tropics and poles. Seasonal changes in the tropics are clearly associated with movement of tropical deep convection and its moistening effect in the upper troposphere [*Tian et al.*, 2006]. Two manifestations of hemispheric asymmetry are also seen in Figure 5. Arctic summer is roughly twice as moist as Antarctic summer at 300 and 250 hPa in Figure 5. Similarly the northern summer subtropics are significantly wetter than southern summer subtropics. This is consistent with stronger monsoon uplift of water vapor in the northern hemisphere.

[26] Figure 6a shows the biases between mean matched AIRS and MLS (AIRS minus MLS) UTWV observations as percentages of $\bar{q}$ in Figure 5. Designated $\bar{\Delta}_q$, this is effectively the relative accuracy (the mean difference) of the AIRS and MLS observations. Figure 6b shows the associated fractional standard deviations of the differences (σ_q) of individual AIRS and MLS matched observations, as percents of $\bar{q}$ in Figure 5. The σ_q in Figure 6b is due to a combination of separate AIRS and MLS measurement system errors, along with errors introduced by the nearest-neighbor matching process described in the Appendix. Assuming measurement errors from AIRS and MLS are uncorrelated, σ_q in Figure 6b is an upper bound on the root-sum-squared precision from MLS and AIRS, for those conditions where both make observations. Of course, the relative errors $\bar{\Delta}_q$ and σ_q cannot be deduced for unmatched observations, so in regions of e.g., 40% yields in Figure 2, Figure 6 tells us nothing about the remaining 60% percent of unmatched retrieval pairs. Therefore Figure 6 is one of several sources of information about MLS and AIRS uncertainties, and it must be interpreted in the context of other validation studies of AIRS and MLS UTWV.

[27] The biases ($\bar{\Delta}_q$) in Figure 6a are generally less than about 5% absolute except at 250 hPa away from the poles. At 300 hPa, MLS is 10–15% drier in middle and low latitudes. Also, at 300 hPa AIRS is wetter over the Antarctic in summer, but 10–20% drier in winter. In the Arctic at 300 hPa AIRS is wetter during the first six months of 2005, but drier during the second six months. (We have not examined whether this holds for other years.) The cause of this is ambiguity in polar regions at 300 hPa is not obvious, but may be related to the climatologies of wet extrema affecting MLS, dry extrema affecting AIRS, behavior of the tropopause not captured by AIRS, or errors in the AIRS-estimated tropopause. In Figure 6b, σ_q at 300 hPa indicates large variability in the AIRS-MLS differences, ranging from 50% at the poles to ±70–80% at low and middle latitudes. *Vömel et al.* [2007] report an MLS dry bias in the tropics of about 25% at 316 hPa, and a slight MLS dry bias in polar regions. *Tobin et al.* [2006] and *Hagan et al.* [2004] show AIRS-radiosonde differences of about ±20% in the tropics at 300 hPa, with *Tobin et al.* [2006] reporting a dry bias of 10–20% in AIRS Version 4.0 data (preliminary, unpublished results by Tobin show

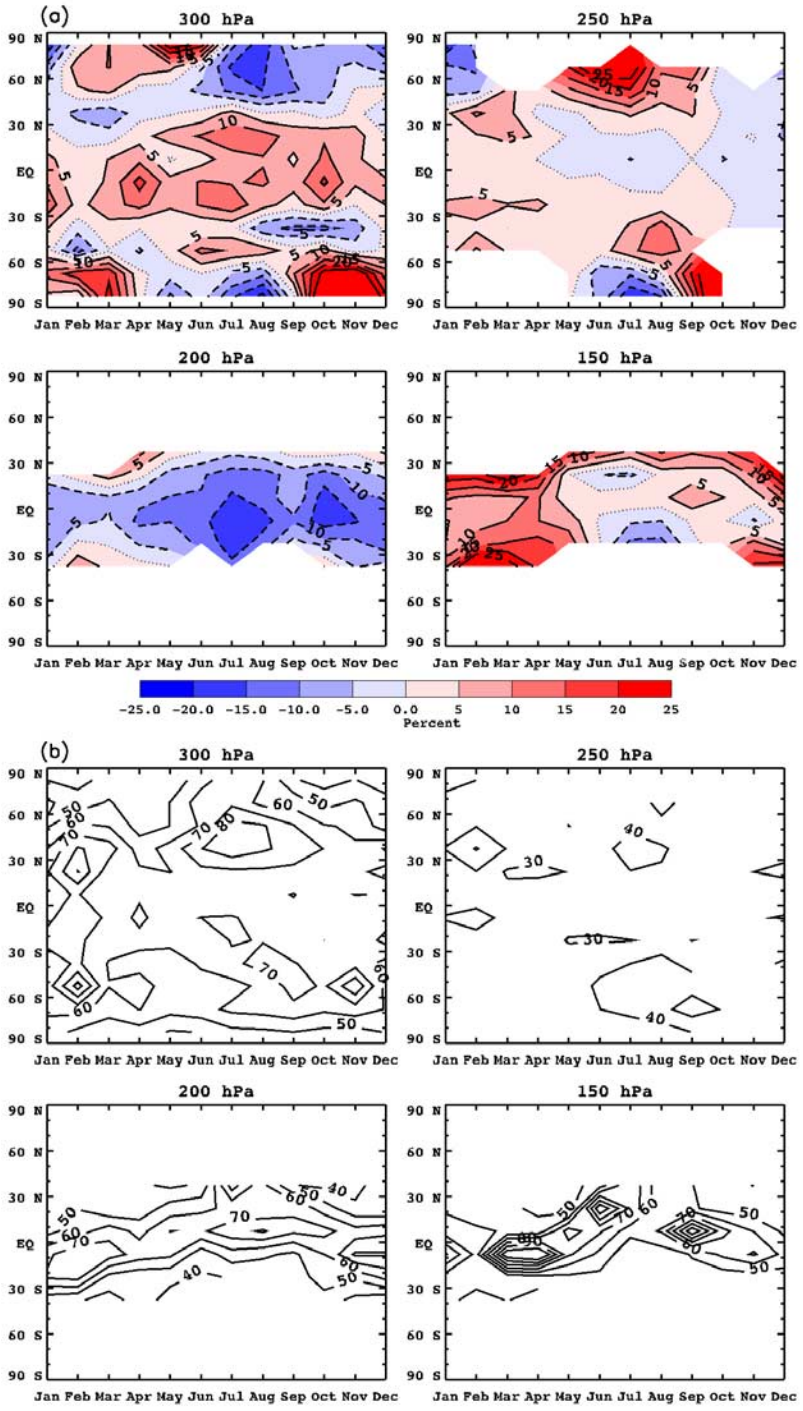

Figure 6. (a) Biases between mean mixing ratios from AIRS and MLS ($\bar{\Delta}_q$) as percentage of means in Figure 5; the zero contour is represented by dotted lines, positive contours are represented by solid lines, and negative contours are represented by dashed lines; contour intervals are 5% for $\leq$15% absolute but otherwise 10%. (b) Standard deviation of the differences of matched MLS and AIRS retrievals pairs (σ_q), as percent of means in Figure 5, with contour intervals of 10%.

smaller biases in AIRS Version 5.0 data). Aircraft comparisons by *Gettelman et al.* [2004] agree with AIRS to ±25%, with no discernable bias at 300 hPa. No validation studies have addressed AIRS UTWV over the poles, though *Gettelman et al.* [2006c] and *Ye et al.* [2007] showed good agreement with sondes at lower levels.

[28] Considering all studies, we interpret Figure 6 at 300 hPa as follows: in the ±45° latitude band MLS is biased low by 10–25% relative to AIRS (consistent with *Vömel et al.* [2007] and $\bar{\Delta}_q$ in Figure 6b), while AIRS itself may be too dry by 10% (consistent with *Tobin et al.* [2006]). Consequently, $\bar{q}$ at 300 hPa in Figure 5 is underestimated

by about 10%. Given an AIRS UTWV precision of ~25% [*Gettelman et al.*, 2004; *Hagan et al.*, 2004; *Tobin et al.*, 2006], we conclude from σ_q in Figure 6b that the MLS precision at 300 hPa is roughly 50% in the ±45° latitude bands. Below we will argue that most of this "uncertainty" comes from differences in how AIRS and MLS respond to UTWV signals, not random error. In short, the two instruments' responses are correlated but their separate responses to UTWV are not one-to-one. At 300 hPa AIRS is drier than MLS by about 10% in northern summer, but wetter by about 10% in southern summer; Because the summer mixing ratios of 60 ppmv or greater at 300 hPa are well within the sensitivity ranges of both instruments, we cannot conclude which instrument is the source of the ~10% ambiguity in absolute UTWV in high-latitude summer. AIRS is slightly wetter than MLS in the winter hemisphere at 300 hPa, reflecting the AIRS tendency toward wetter UTWV estimate under the driest conditions. *Vömel et al.* [2007] find CFH sondes to be ~10% wetter than MLS in Arctic winter. The σ_q in Figure 6b at 300 hPa puts an upper bound on the two instruments' precision at high latitudes: they are both somewhere in the 25 to 40% range at 300 hPa, assuming a reasonable lower limit of about 25%. Note that this high-latitude estimate of precision is an overestimate because it assumes the nearest-neighbor matching procedure introduces no uncertainty.

[29] The situation at 250 hPa is much clearer than at 300 hPa. Figure 6a shows essentially zero bias ($\bar{\Delta}_q$), except in high-latitude summer where AIRS is wetter by 10–20%, and high-latitude winter where AIRS is drier by 10–20%. As $\bar{q}$ in Figure 5 shows, this AIRS moist bias occurs where UTWV is near the AIRS sensitivity threshold of 15–20 ppmv, implying that polar UTWV values at 250 hPa are usually below the AIRS sensitivity threshold. Values of σ_q at 250 hPa in Figure 6b are everywhere 40% or less, implying individual instrument precisions of 20–30% at 250 hPa. We conclude that UTWV at 250 hPa from either AIRS or MLS, at all but highest latitudes, are correct to within ±25%, with a dry bias of 10% or less by both instruments (supported by *Vömel et al.* [2007] for MLS and *Tobin et al.* [2006] for AIRS). At highest latitudes, AIRS uncertainties at 250 hPa are greater than 30%, probably because of the prevalence of drier conditions there. In summary, Figure 6 indicates remarkable agreement between AIRS and MLS water vapor measurements at 250 hPa except when mixing ratios are near the AIRS sensitivity limit of 15–20 ppmv. At those lowest mixing ratios AIRS shows a consistent wet bias.

[30] At 200 hPa both $\bar{\Delta}_q$ and σ_q are considerably larger than at 250 hPa. Values of $\bar{\Delta}_q$ in Figure 6a show that MLS is wetter than AIRS by 5–15% at 200 hPa, opposite to the situation at 300 hPa. Although *Read et al.* [2007] did not find such large differences as shown here, they rejected all matches where MLS UTWV is 20 ppmv or less. *Read et al.* [2007] were not able to devise an AIRS-only rejection threshold that gives good agreement with MLS. We report the complete comparison statistics because this screening method is not viable for the roughly 99% of AIRS footprints that do not match to an MLS sounding. This will aid in interpretation of the entire AIRS data volume. Values of σ_q at 200 hPa in Figure 6b range from 40 to 70%, and examination of the 200 hPa $\bar{q}$ in Figure 5 shows these large uncertainties are associated with mean mixing ratios of 10–60 ppmv. This is close to, or below, the 15–20 ppmv sensitivity threshold for AIRS. Furthermore, *Vömel et al.* [2007] show improved agreement between MLS and CFH measurements for drier conditions (with the best agreement seen for mixing ratios of roughly 3 to 10 ppmv; *Lambert et al.* [2007]). We therefore conclude that the most likely explanation of large values for both $\bar{\Delta}_q$ and σ_q in Figure 6 at 200 hPa is AIRS insensitivity to drier conditions. This implies the AIRS uncertainties at 200 hPa are roughly −10 to −20 ± 40 to 60%. Similar arguments hold for the $\bar{\Delta}_q$ values of −10 to +20, and σ_q values of 50–90% at 150 hPa. The MLS uncertainties at these pressure were shown to be ~25% by *Vömel et al.* [2007], so $\bar{\Delta}_q$ and σ_q in Figures 6a and 6b are the effective AIRS uncertainties at 150 hPa. As will be shown below, correlations between AIRS and MLS at 200 and 150 hPa are small though significantly larger than zero, suggesting AIRS has some skill even at these pressures. Also, the AIRS performance will be significantly better than the zonal mean value in Figure 6 wherever local UTWV is above approximately 15 ppmv, though poorer where UTWV is locally small.

3.4. Extrema

[31] The previous section described the zonal mean agreement between the AIRS and MLS differences. Another important requirement for creating climatologies from the two instruments is understanding how they sample dry and moist extrema. Extrema are also significant in determining correlations between data. Note, however, that even perfect agreement in probability distributions does not guarantee that one or both instruments have skill, since they may simply be defaulting to similar climatologies. For this reason section 3.5 below shows correlations between the two data sets.

[32] Figure 7a gives the third percentile of MLS observations ($q_{MLS-3\%}$). These represent the driest 3% of scenes observed by MLS. A comparison of $q_{MLS-3\%}$ in Figure 7a with $\bar{q}$ in Figure 5 shows the maxima in both fields are collocated, and both fields diminish poleward. Note, however, that the ratio of the quantities in Figures 7a and 5 ($q_{MLS-3\%}$: $\overline{q}$) varies from ~10% at 300 hPa in the tropics to ~40% at 150 hPa. This indicates lower variability with increasing height. That ratio is also smaller at higher latitudes. Higher fractional variability at lower latitudes and altitudes suggest larger effects of deep convection at 300 hPa. Interestingly, fields of $q_{MLS-3\%}$ at 300 and 250 hPa in Figure 7a are very similar despite a roughly threefold decrease in $\bar{q}$ between these two levels in Figure 5. It is unclear whether this is an artifact of the MLS retrieval or a true characteristic of the atmosphere.

[33] Figure 7b shows the third percentile, or driest 3%, of AIRS observations, but as a percentage of $q_{MLS-3\%}$ in Figure 7a (designated $\%_{AIRS-3\%}$ to signify percentage). Note that if MLS and AIRS have similar lower limit sampling, then $\%_{AIRS-3\%}$ in Figure 7b would be roughly 100% everywhere. Instead, $\%_{AIRS-3\%}$ is generally larger than 100%. At 300 hPa $\%_{AIRS-3\%}$ is never smaller than 150%, so the driest scenes from AIRS are always wetter than those from MLS. Note, however, that $q_{MLS-3\%}$ at 300 hPa in Figure 7a is everywhere near the putative 15–20 ppmv sensitivity threshold of AIRS, and that AIRS

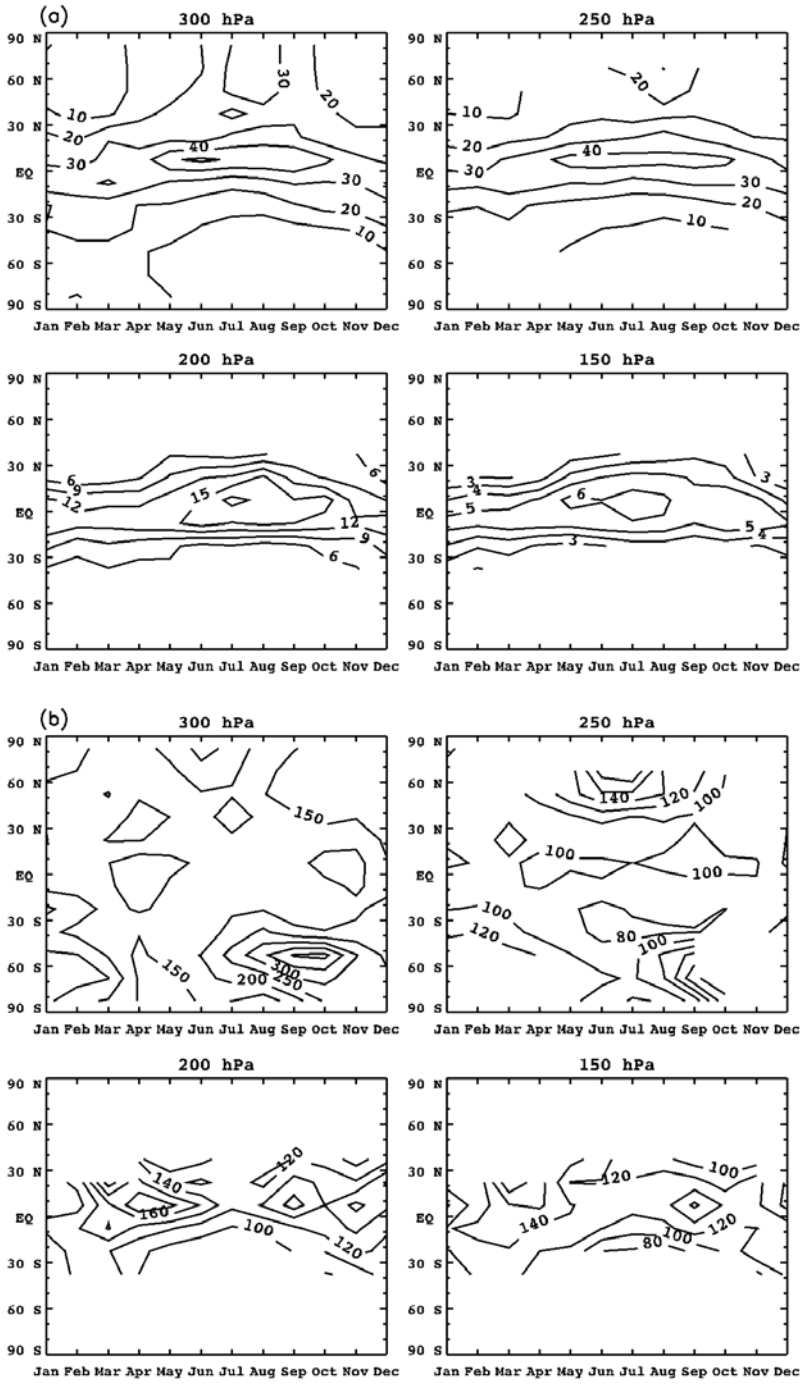

Figure 7. Value of the (a) third percentile (driest 3%) of MLS observations in ppmv ($q_{MLS-3\%}$) and the (b) third percentile of AIRS UTWV ($\%_{AIRS-3\%}$) as percent of MLS values in Figure 7a.

cannot observe these very dry conditions. Furthermore, the possibly unrealistic near-equivalence of $q_{MLS-3\%}$ at 300 and 250 hPa in Figure 7a suggests problems with MLS for very driest scenes at 300 hPa. Therefore we can conclude little about the occurrence of very dry air at 300 hPa in the tropics and subtropics from either AIRS or MLS. In contrast, values of $\%_{AIRS-3\%}$ at 250 hPa in Figure 7b are very close to 100% throughout the tropics and subtropics. This is yet more evidence that AIRS and MLS sample UTWV very similarly at 250 hPa. Note, however, that $q_{MLS-3\%}$ at 250 hPa in Figure 7a is 20–30 ppmv—close to but slightly higher than the AIRS lower limit sensitivity threshold—in regions where $\%_{AIRS-3\%}$ is close to 100%. At 150 and 200 $\%_{AIRS-3\%}$ is almost always 120% or greater, meaning driest AIRS scenes are not as dry as driest MLS scenes. This reflects the tendency for AIRS to relax to climatology under very dry conditions, an effect most pronounced in the lower stratosphere where AIRS has no skill except in the mean.

[34] Figure 8a shows the 97th percentile of MLS observations ($q_{MLS-97\%}$) in ppmv. These represent the wettest 3% of scenes observed by MLS. Comparison with $\bar{q}$ in Figure 5 shows maxima several times larger than the means, though

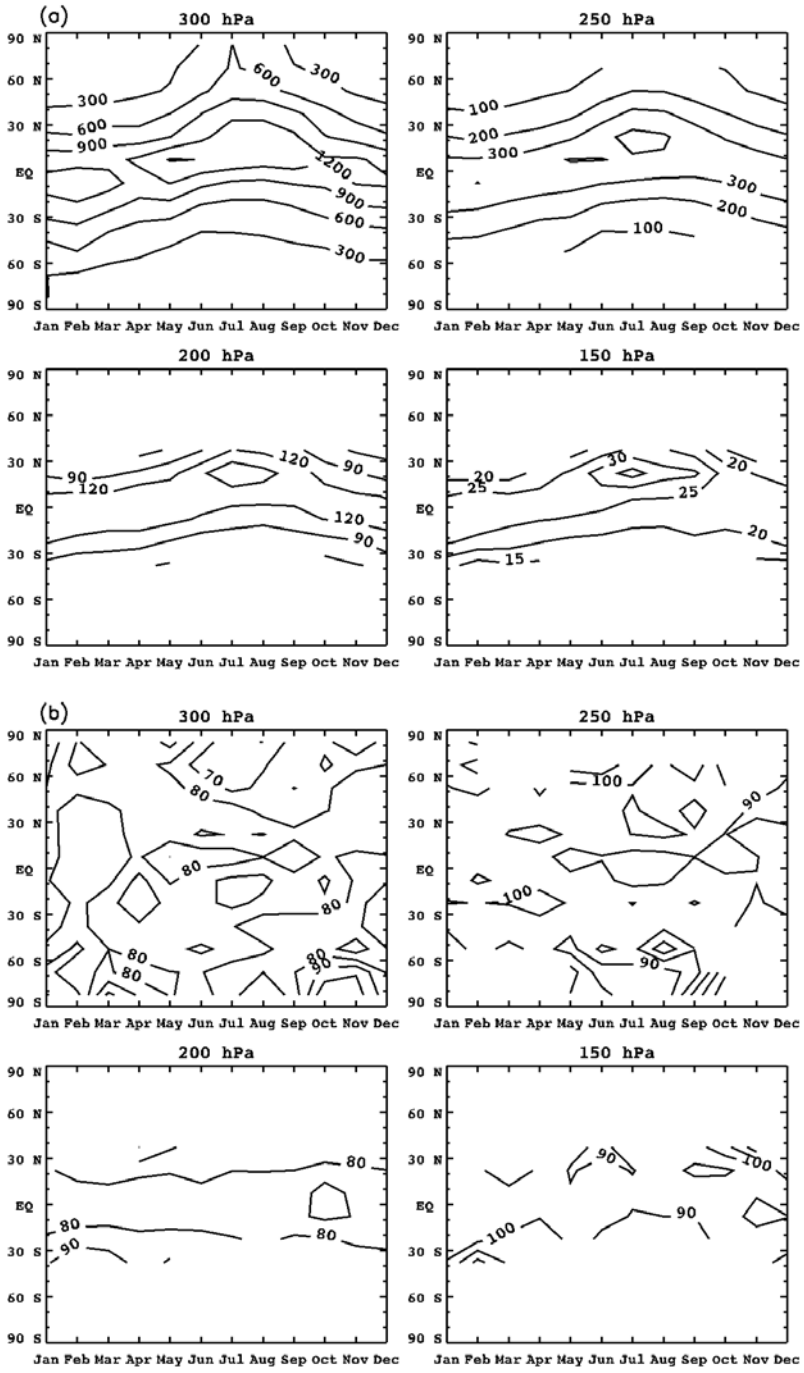

Figure 8. Value of the (a) 97th percentile (wettest 3%) of MLS observations ($q_{MLS-97\%}$) in ppmv and the (b) 97th percentile of AIRS observations ($\%_{AIRS-97\%}$) as percent of MLS values in Figure 8a.

the ratio $q_{MLS-97\%}$: $\bar{q}$ varies from about 4:1 to 6:1 at 300 hPa to about 2:1 at 150 hPa. Recall that the dynamic range of $q_{MLS-3\%}$ similarly decreased with pressure. This indicates that the magnitude and fractional variability of UTWV are both largest at 300 hPa. Figure 8b gives the 97th percentile of AIRS observations as a percentage of $q_{MLS-97\%}$ (defined as $\%_{AIRS-97\%}$). Figure 8b shows that AIRS maxima are almost always smaller than those of MLS at 300 and 200 hPa. Overall, AIRS has drier maxima than MLS at low latitudes, with maxima above the roughly 15–20 ppmv AIRS sensitivity threshold everywhere at 300 hPa, and in the moist tropics at 250 and 200 hPa. Smaller AIRS maxima are further supported by the 90th percentile plot (not shown), analogous to $\%_{AIRS-97\%}$ in Figure 8b but everywhere smaller than Figure 6a. This shows that the larger the value of an observation, the higher the probability of MLS being wetter than AIRS, consistent with the findings of *Read et al.* [2007]. A tendency toward the mean in AIRS is noted by *McMillin et al.* [2007] in their comparison of AIRS total precipitable water vapor with ground-based sensors; a

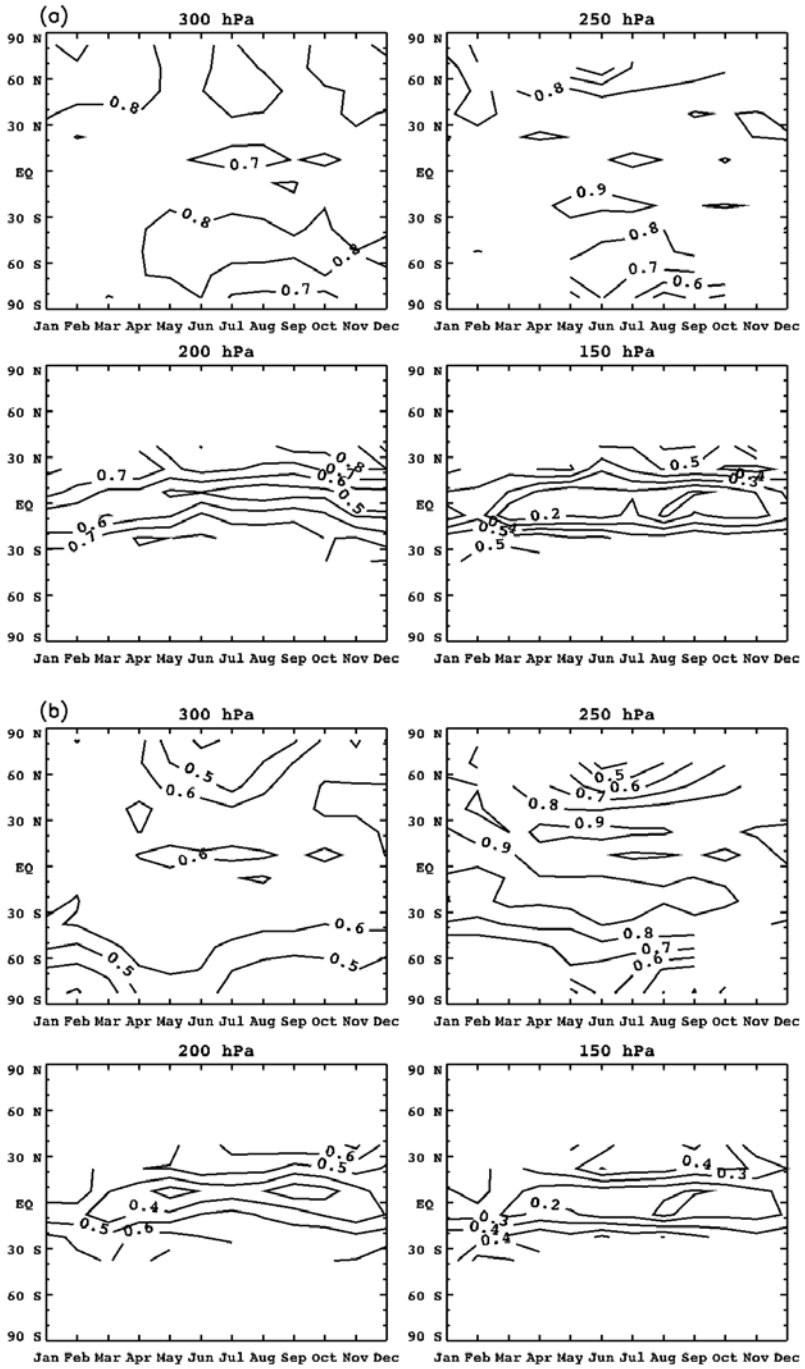

Figure 9. (a) Pearson correlation coefficients between AIRS and MLS UTWV values (ρ). (b) Slope of linear fit of AIRS to MLS data (m).

similar effect may be occurring for AIRS UTWV observations. However, as argued by *Read et al.* [2007], MLS tends to overestimate scenes wetter than 400 ppmv. So, the RMS differences seen at 300 hPa in Figure 4b are most likely due to MLS overestimation of water vapor for the wettest conditions.

3.5. Correlation Coefficients and Linearity

[35] The linear (Pearson) correlation coefficients between AIRS and MLS UTWV (designated ρ) for the twelve months, twelve zonal bands and four pressures are shown in Figure 9a. The slope of the least squares fitted line (m) is shown in Figure 9b. AIRS is treated as the dependent variable in the line fitting here, so m values less than unity imply AIRS has smaller maxima and/or larger minima. The highest correlations in Figure 9a (greater than 0.9) are found at 250 hPa, with a rapid decrease at upper levels. Note, however, that the fitted MLS-AIRS linear slope is always 0.9 or less. The bias toward smaller m is consistent with the extrema just discussed, with AIRS having a smaller dynamic

range than MLS. Purely random measurement noise would give a mean m of unity, with some variations about that.

[36] At 300 hPa, ρ in Figure 9a is relatively high (0.7 to 0.8), while m in Figure 9b is 0.5–0.6. The relative errors shown in Figure 2 at 300 hPa, and the extrema discussed with Figures 7 and 8 above explain this apparent discrepancy. At 300 hPa MLS tends to measure wetter than AIRS when wet, and drier than AIRS when dry. This is consistent with the smaller values of m in Figure 9b. However the high correlation in Figure 9a at 300 hPa suggests that MLS has sensitivity at this level, though a different response to UTWV than AIRS. *Vömel et al.* [2007] similarly find MLS is responsive to geophysical signal but does not respond in the same manner as the balloon-borne CFH sensors at 316 hPa. Figure 9 explains the relatively large RMS differences at 300 hPa seen in Figure 6: while the two data sets are monotonically related to one another, that relationship is not one-to-one, leading to larger RMS differences.

[37] The highest correlation in Figure 9a is seen at 250 hPa, where ρ is as large as 0.9. Note, however, that the fitted slope m at 250 hPa has a maximum of 0.9; no values of m at 250 hPa (or anywhere else) exceeds unity. The explanation for this is found in Figure 8a: AIRS maxima at 250 hPa are always 100% or less of MLS maxima. Because both correlation coefficients and slope calculations use least squares fitting, both are influenced heavily by the largest values [*Wilks*, 2006]. Moving upward, at 200 hPa the correlation ρ in Figure 9a continues to decrease to 0.5–0.8 at 200 hPa, while the fitted slope m in Figure 9b is only 0.4 to 0.6. Again the explanation for this weaker linearity is lower extrema for AIRS (as discussed above with Figures 7 and 8). The poorer correlation at 200 hPa is due to increasing AIRS uncertainty. Note that minimum ρ at 200 hPa near the equator during September is inconsistent with putatively better AIRS sensitivity for moderately wet conditions, suggesting a suboptimal retrieval method for AIRS at the lowest limits of its sensitivity at 200 hPa. Finally, at 150 hPa, ρ is only 0.2–0.5. While small, a correlation coefficient of 0.5 suggests AIRS has some skill at 150 hPa. However, m is only 0.2–0.4 at 150 hPa, suggesting that AIRS skill is confined to only the very wettest scenes. Examination of scatter plots of AIRS and MLS 150 hPa water vapor supports this conclusion.

4. Summary and Conclusions

[38] This work takes several steps toward providing a complete and representative UTWV climatology from AIRS and MLS. Several of the conclusions reached here are consistent with earlier studies of UTWV derived from AIRS and MLS, especially those of *Read et al.* [2007] and *Vömel et al.* [2007]. Examples of corroborations of earlier results are: an AIRS sensitivity threshold around 15–20 ppmv [*Gettelman et al.*, 2004], an MLS dry bias of 10–20% at 300 hPa, a tendency for MLS to be responsive to the wettest scenes but overestimating the largest values, and best agreement at 250 hPa in the tropics. Some aspects of this study have not been examined in earlier studies, especially the two instrument's sampling variations by month and latitude as shown in Figure 2. Notably, both instruments preferentially sample clear scenes in the tropics, while MLS is completely unaffected by clouds poleward of ±45° latitude. Also, the AIRS performance decreases rapidly above about 200 hPa, likely because of the increasing prevalence of dry conditions with altitude. This is near the nominal lower extent of the tropical tropopause layer, where convection reaches its upper limits [*Gettelman and Forster*, 2002].

[39] The results of this study are summarized in Tables 2 and 3, broadly divided between lower latitude climate regimes where AIRS samples the entire troposphere (Table 2), and higher latitudes where a lowered tropopause usually precludes AIRS observations at 200 and 150 hPa (Table 3). While our estimates of biases and standard deviations are sometimes as large as 20% and 90%, respectively, correlation is a more fundamental measure of agreement. Tables 2 and 3 show correlations of 0.7 or greater everywhere at 300 and 250 hPa, and throughout the tropics at 200 hPa. This high correlation suggests that both AIRS and MLS are responsive to prevalent UTWV amounts throughout most of the upper troposphere, and certainly in those locations with roughly 20 to 400 ppmv of water vapor. However, the two instrument's responses with UTWV amount may be different. (AIRS stratospheric water vapor "observations" have only climatological information, and essentially zero correlation with MLS observations.) Small errors in the spectroscopy used in the forward models in each instrument's retrieval system are a plausible explanation for this apparent discrepancy between correlation in Figure 9 and RMS differences in Figure 6b. *Read et al.* [2007] ascribe shortcomings in UTWV from MLS at 316 hPa to spectral calibration and transmission uncertainties of ~1%, and similar effects may be at work in the AIRS retrieval system. The AIRS spectroscopic validation is described by *Strow et al.* [2003, 2006].

[40] The results shown here are relevant to several published studies. As noted here and by *Vömel et al.* [2007] and *Read et al.* [2007], MLS overestimates UTWV in the wettest scenes. *Su et al.* [2006a, 2006b] determine water vapor and cloud feedbacks by relating the logarithm of total UTWV in the 316–100 hPa layer (dominated by the 316 hPa value), the logarithm of mean MLS cloud ice amounts, and sea surface temperature (SST). MLS has sensitivity to UTWV at pressures considered here (although that sensitivity is not linear with AIRS sensitivity at 300 hPa). Also, the inferred feedback relationships are logarithmic in changes in UTWV. Therefore the fundamental results of *Su et al.* [2006a, 2006b] are likely unchanged: water vapor and cloud feedbacks increase with SST. However, the amplitude of that change will be modified with MLS water vapor at 316 hPa as transmissivities are corrected in later data versions. Importantly, changes in estimated feedback strength will be proportional to the changes in the logarithm of the MLS water vapor. Also, *Gettelman et al.* [2006a, 2006b] examined relative humidity climatologies, including those in the 200 hPa layer in the tropics. These studies focus mainly on saturation and near-saturation conditions, associated with highest water vapor loading. Figure 8 suggests that AIRS may be underestimating the 200 hPa water vapor for wettest scenes, so that regions of supersaturation noted by *Gettelman et al.* [2006a, 2006b] may be more extensive than described there.

Table 2. Summary of Results for Tropics and Latitude to About 45 Degrees in the Summer Hemisphere[a]

		Pressure			
		300 hPa	250 hPa	200 hPa	150 hPa
Estimated uncertainties (from $\bar{\Delta}_q$, σ_q and extrema) (%)	MLS	10 ± 40–60%	±25%	±25%	±25%
	AIRS	±25%	±25%	−10 ± 50–70%	5 ± 50–90%
Correlation coefficient (ρ)		0.7–0.8	0.9	0.5–0.8 (AIRS uncertainties)	0.2–0.4 (high AIRS uncertainties)
Fitted slope (m)		0.4–0.5 (skewed by wettest MLS scenes)	0.7–0.8 (fewer AIRS extrema)	0.1–0.2 (fewer AIRS extrema)	0.1–0.2 (small AIRS sensitivity at this pressure)
		Effect of Clouds on Yields			
MLS		MLS retrieval yields range from ~50% in regions of deep convection to near 100% in the regions of prevalent low clouds (trade cumulus and stratocumulus).			
AIRS		AIRS yields range from 15% in regions of deep convection and prevalent stratocumulus [see *Fetzer et al.*, 2006] to 90% in trade wind cumulus.			

[a]Retrieval yields, and listed variables $\bar{\Delta}_q$, σ_q, extrema, ρ, and m are discussed more completely in the text.

[41] The effects of cloud-induced sampling in UTWV measurements from both MLS and AIRS remain unresolved in this work. Even cursory examination of the two instruments' yields suggest that cloud-induced sampling biases may have important implications for any study with MLS or AIRS UTWV in the moist tropics [e.g. *Su et al.*, 2006a, 2006b; *Gettelman et al.*, 2006a, 2006b; *Dessler and Minschwaner*, 2007]. Characterizing those biases (if indeed they exist) will be challenging, requiring correlative information about water vapor both inside and outside clouds over scale of tens to hundreds of kilometers.

Appendix A: Quality Control and Data Matching

[42] The AIRS quality control for the Version 4.0 data is essentially determined by the cloud cover in a scene [*Susskind et al.*, 2006; *Fetzer et al.*, 2006]. Here we use the flag *Qual_Temp_Profile_Mid* = 0 to exclude those very cloudy AIRS profiles whose UTWV retrievals are retrieved solely from AMSU microwave observations [*Tobin et al.*, 2006; *Susskind et al.*, 2006]. This quality control gives AIRS water vapor profiles covering the entire upper troposphere.

[43] The MLS version 1.5 UTWV observations are screened by criteria described by *Livesey et al.* [2006a]: *Status* is an even number, *Quality* > 5.0 at 316 hPa and *Quality* > 0.3 at 215 hPa and lower pressures. Note that these criteria yield some partial MLS profiles, where the 316 hPa level is flagged as lower quality. This affects about 10% of MLS profiles in the tropics, while all MLS profiles are intact at higher latitudes.

[44] In this study we match MLS and AIRS UTWV observations horizontally with a nearest-neighbor method. This approach is taken for two reasons, both related to formulation of the AIRS and MLS retrieval algorithms. First, techniques for comparing different remote sensing instruments assume their retrieval algorithms provide reliable estimates of information content as either averaging kernels [*Rodgers and Connor*, 2003] or measurement uncertainties [*Read et al.*, 2006]. While the MLS retrieval algorithm provides these quantities, the AIRS Version 4.0 retrieval algorithm considered here does not. Consequently, a formal error-weighted smoothing is not feasible for the data version considered here. AIRS Version 5.0 data report averaging kernels, but their utility has not been fully assessed. The results shown here are necessarily an approximation to the more optimal approaches.

[45] The second reason for using a nearest-neighbor matching method is related to the categorical nature of quality criteria for both systems. The ultimate objective of this comparison is to account for all scenes mutually viewed by both instruments, including those not available from one or both instruments because of retrieval quality criteria described earlier. The nearest-neighbor method allows the preservation of quality flagging in the matching process, something less straightforward with horizontal smoothing or interpolation. *Froidevaux et al.* [2006] used a nearest-neighbor horizontal matching and MLS vertical averaging kernels to smooth the AIRS profiles. *Read et al.* [2007] used horizontal smoothing based on MLS error estimates only (as described by *Read et al.* [2006]) to obtain a more optimal match between AIRS and MLS. As in this study, Read et al. accomplished vertical matching by fitting AIRS to MLS reference pressures using geometric means of the AIRS profiles. Note that the horizontal smoothing used by Read et al. is essentially a weighted average over several adjacent AIRS profiles, using only that subset of AIRS profiles with highest quality retrievals. Similarly, Read et al. did not

Table 3. As Table 2 for Conditions Poleward of About 45 Degrees Latitude in the Summer Hemisphere and About 30 Degrees Latitude in the Winter Hemisphere

		Pressure	
		300 hPa	250 hPa
Estimated uncertainties (from $\bar{\Delta}_q$, σ_q and extrema) (%)	MLS	±25–40%	±25%
	AIRS	±25–40%	±25–40%
Correlation coefficient (ρ)		0.7–0.8	0.7–0.8
Fitted slope (m)		0.2–0.4 (skewed by wettest MLS scenes and driest AIRS scenes)	0.2–0.6 (skewed by zAIRS insensitivity to driest scenes)
		Effect of Clouds on Yields	
MLS		MLS yields are nearly 100% within and poleward of the tropopause break at the jet stream.	
AIRS		AIRS yields are typically 30-60% poleward of the tropopause break.	

match non-convergent MLS retrievals to any AIRS retrieval. Here we consider scenes with both convergent and non-convergent solutions.

[46] We compare UTWV mixing ratios on the 300, 250, 200 and 150 hPa levels (not the layer means, as reported for AIRS). MLS reports level values at 316, 215, 147 and 100 hPa, and the MLS retrieval algorithm is formulated so the logarithm of mixing ratio is linear in logarithm of pressure [*Livesey et al.*, 2006a]. The MLS observations are placed on the reference pressures of 400, 300, 250, 200 and 100 hPa using this functional relationship between MLS UTWV and pressure. This preserves the vertical resolution of MLS UTWV, as discussed by *Waters et al.* [2006] and *Livesey et al.* [2006b].

[47] The AIRS Version 4.0 data are reported as log-pressure-weighted mean values within layers. The AIRS layer indexing is such that the reference pressure is the higher of the bracketing pressures; e.g., $\bar{q}(p = 300)$ represents the 300–250 hPa layer average. The index decreases with pressure. We assume linear variations of the logarithm of mixing ratio with the logarithm of pressure, and use geometric means to calculate the level values between layers $q_{AIRS}(p_i) = \sqrt{\bar{q}_{AIRS}(p_i)\bar{q}_{AIRS}(p_{i-1})}$. Here $\bar{q}_{AIRS}(p_i)$ is the reported layer average value and $q_{AIRS}(p_i)$, is the geometric mean used in this study. This requires layers values reported at 400, 300, 250, 200 and 150 hPa (bracketing our pressure levels of 300, 250, 200 and 150 hPa).

[48] As with the nearest neighbor method used to match in the horizontal, this vertical matching is not formally optimal [*Rodgers and Connor*, 2003]. However, the MLS vertical resolution is about 2.7 km (the grid spacing), while AIRS vertical resolution in the upper troposphere is similar [*Maddy and Barnet*, 2008]. Both instruments' resolutions are close to the water vapor e-folding height of 2–3 km. We postulate that the vertical matching procedure used here does not introduce large errors; basically neither instrument's fine-scale structure contributes significantly to the RMS differences. The RMS differences between AIRS and MLS at 250 hPa are 30% everywhere except the poles, comparable to the differences seen by *Read et al.* [2007] when more formal horizontal matching procedures are used. This suggests that AIRS and MLS are individually performing to better than 25% RMS uncertainty at 250 hPa. Regions of poorer agreement can be best explained by reduced performance by either AIRS for driest conditions, or MLS for wettest conditions.

[49] **Acknowledgments.** The research described in this paper was carried out at the Jet Propulsion Laboratory, California Institute of Technology, under a contract with the National Aeronautics and Space Administration. It was supported by the AIRS and MLS projects at JPL and by the NASA and Energy and Water-cycle Study (NEWS) project. We benefited from conversations with Darryn Waugh, Andrew Gettelman, Jim Yoe, M. K. Rama Varma Raja, Bill Randel, Mijeong Park, George Aumann, and Evan Fishbein.

References

Aumann, H. H., et al. (2003), AIRS/AMSU/HSB on the Aqua mission: Design, science objectives, data products and processing system, *IEEE Trans. Geosci. Remote Sens.*, *41*, 253–264.

Betts, A. K. (1973), A composite mesoscale cumulonimbus budget, *J. Atmos. Sci.*, *30*, 597–610.

Bony, S., et al. (2006), How well do we understand and evaluate climate change feedback processes?, *J. Clim.*, *19*, 3445–3448.

Dessler, A. E., and K. Minschwaner (2007), An analysis of the regulation of tropical tropospheric water vapor, *J. Geophys. Res.*, *112*, D10120, doi:10.1029/2006JD007683.

Divakarla, M., C. Barnet, M. D. Goldberg, L. McMillin, E. S. Maddy, W. W. Wolf, L. Zhou, and X. Liu (2006), Validation of Atmospheric Infrared Sounder temperature and water vapor retrievals with matched radiosonde measurements and forecasts, *J. Geophys. Res.*, *111*, D09S15, doi:10.1029/2005JD006116.

Eguchi, N., and M. Shiotani (2004), Intraseasonal variations of water vapor and cirrus clouds in the tropical upper troposphere, *J. Geophys. Res.*, *109*, D12106, doi:10.1029/2003JD004314.

Ferrare, R. A., et al. (2004), Source characterization of upper-troposphere water vapor measurements during AFWEX using LASE, *J. Atmos. Ocean. Technol.*, *21*, 1790–1808.

Fetzer, E. J., J. Teixeira, E. Olsen, and E. Fishbein (2004), Satellite remote sounding of atmospheric boundary layer temperature inversions over the subtropical eastern Pacific, *Geophys. Res. Lett.*, *31*, L17102, doi:10.1029/2004GL020174.

Fetzer, E. J., B. H. Lambrigtsen, A. Eldering, H. H. Aumann, and M. T. Chahine (2006), Biases in total precipitable water vapor climatologies from Atmospheric Infrared Sounder and Advanced Microwave Scanning Radiometer, *J. Geophys. Res.*, *111*, D09S16, doi:10.1029/2005JD006598.

Folkins, I., and R. V. Martin (2005), The vertical structure of tropical convection, and its impact on the budgets of water vapor and ozone, *J. Atmos. Sci.*, *62*, 1560–1573.

Froidevaux, L., et al. (2006), Early validation analyses of atmospheric profiles from EOS MLS on the Aura satellite, *IEEE Trans. Geosci. Remote Sens.*, *44*(5), 1106–1121.

Fu, R., Y. Hu, J. S. Wright, J. H. Jiang, R. E. Dickinson, M. Chen, M. Filipiak, W. G. Read, J. W. Waters, and D. L. Wu (2006), Short circuit of water vapor and polluted air to the global stratosphere by convective transport over the Tibetan Plateau, *Proc. Natl. Acad. Sci. U.S.A.*, *103*, 5664–5669.

Gettelman, A., and P. M. de F. Forster (2002), A climatology of the tropical tropopause layer, *J. Meteorol. Soc. Jpn.*, *80*(4B), 911–924.

Gettelman, A., et al. (2004), Validation of Aqua satellite data in the upper troposphere and lower stratosphere with in-situ aircraft instruments, *Geophys. Res. Lett.*, *31*, L22107, doi:10.1029/2004GL020730.

Gettelman, A., W. D. Collins, E. J. Fetzer, A. Eldering, and F. W. Irion (2006a), A satellite climatology of upper tropospheric relative humidity and implications for climate, *J. Clim.*, *23*, 6104–6121.

Gettelman, A., E. J. Fetzer, A. Eldering, and F. W. Irion (2006b), The global distribution of supersaturation in the upper troposphere from the Atmospheric Infrared Sounder, *J. Clim.*, *23*, 6089–6103.

Gettelman, A., V. P. Walden, L. M. Miloshevich, W. L. Roth, and B. Halter (2006c), Relative humidity over Antarctica from radiosondes, satellites, and a general circulation model, *J. Geophys. Res.*, *111*, D09S13, doi:10.1029/2005JD006636.

Hagan, D. E., C. R. Webster, C. B. Farmer, R. D. May, R. L. Herman, E. M. Weinstock, L. E. Christensen, L. R. Lait, and P. A. Newman (2004), Validating AIRS upper atmosphere water vapor retrievals using aircraft and balloon in situ measurements, *Geophys. Res. Lett.*, *31*, L21103, doi:10.1029/2004GL020302.

Hartmann, D. L., and K. Larson (2003), An important constraint on tropical cloud—Climate feedback, *Geophys. Res. Lett.*, *29*(20), 1951, doi:10.1029/2002GL015835.

Hearty, T. J., E. T. Olsen, E. Fetzer, S.-Y. Lee, E. Fishbein, W. F. Irion, B. Kahn, E. Manning, S. Granger, and B. Tian (2007), AIRS/AMSU/HSB Version 5 Level 2 Performance and Test Report. (Available at http://disc.sci.gsfc.nasa.gov/AIRS/documentation/v5_docs/v5_docs_list.shtml)

Held, I., and B. J. Soden (2000), Water vapor feedback and global warming, *Annu. Rev. Energy Environ.*, *25*, 441–475.

Highwood, E. J., and B. J. Hoskins (1998), The tropical tropopause, *Q. J. R. Meteorol. Soc.*, *124*, 1579–1604.

Holton, J. R., and A. Gettelman (2001), Horizontal transport and the dehydration of the stratosphere, *Geophys. Res. Lett.*, *28*, 2799–2802.

Holton, J. R., P. H. Haynes, M. E. McIntyre, A. R. Douglass, R. B. Rood, and L. P. Pfister (1995), Stratosphere-Troposphere exchange, *Rev. Geophys.*, *33*, 405–439.

Jensen, E. J., and A. S. Ackerman (2006), Homogeneous aerosol freezing in the tops of high-altitude tropical cumulonimbus clouds, *Geophys. Res. Lett.*, *33*, L08802, doi:10.1029/2005GL024928.

Jensen, E. J., et al. (2000), Prevalence of ice supersaturated regions in the upper troposphere: Implications for optically thin ice cloud formation, *J. Geophys. Res.*, *106*, 17,253–17,266.

Kahn, B. H., C. K. Liang, A. Eldering, A. Gettelman, Q. Yue, and K.-N. Liou (2008), Tropical thin cirrus and relative humidity observed by the Atmospheric Infrared Sounder, *Atmos. Chem. Phys. Discuss.*, *7*, 16,185–16,225.

Kärcher, B., and W. V. Lohmann (2003), A parameterization of cirrus cloud formation: Heterogeneous freezing, *J. Geophys. Res.*, *108*(D14), 4402, doi:10.1029/2002JD003220.

Lambert, A., et al. (2007), Validation of the Aura Microwave Limb Sounder middle atmosphere water vapor and nitrous oxide measurements, *J. Geophys. Res.*, *112*, D24S36, doi:10.1029/2007JD008724.

Lambrigtsen, B. H. (2003), Calibration of the AIRS microwave instruments, *IEEE Trans. Geosci. Remote Sens.*, *41*, 369–378.

L'Ecuyer, T. S., and G. L. Stephens (2003), The tropical oceanic energy budget from the TRMM perspective. part I: Algorithm and uncertainties, *J. Clim.*, *16*, 1967–1985.

Lin, B., B. A. Wielicki, P. Minnis, L. Chambers, K. M. Xu, Y. X. Hu, and A. Fan (2006), The effect of environmental conditions on tropical deep convective systems observed from the TRMM satellite, *J. Clim.*, *19*, 5745–5761.

Liu, C. (2007), Geographical and seasonal distribution of tropical tropopause thin clouds and their relation to deep convection and water vapor viewed from satellite measurements, *J. Geophys. Res.*, *112*, D09205, doi:10.1029/2006JD007479.

Liu, C., E. Zipser, T. Garrett, J. H. Jiang, and H. Su (2007), How do the water vapor and carbon monoxide "tape recorders" start near the tropical tropopause?, *Geophys. Res. Lett.*, *34*, L09804, doi:10.1029/2006GL029234.

Livesey, N. J., et al. (2006a), Earth Observing System (EOS) Microwave Limb Sounder (MLS) Version 1.5 Level 2 Data Quality and Description Document. (Available at http://mls.jpl.nasa.gov/)

Livesey, N. J., W. V. Snyder, W. G. Read, and P. A. Wagner (2006b), Retrieval algorithms for the EOS Microwave Limb Sounder (MLS) instrument, *IEEE Trans. Geosci. Remote Sens.*, *44*(5), 1144–1155.

Maddy, E. S., and C. D. Barnet (2008), Vertical resolution estimates in Version 5 of AIRS operational retrievals, *IEEE Trans. Geosci. Remote Sens.*, in press.

Massie, S. T., A. Heymsfield, C. Schmitt, D. Müller, and P. Seifert (2007), Aerosol indirect effects as a function of cloud top pressure, *J. Geophys. Res.*, *112*, D06202, doi:10.1029/2006JD007383.

McMillin, L. M., J. Zhao, M. K. Rama Varma Raja, S. I. Gutman, and J. G. Yoe (2007), Radiosonde humidity corrections and potential Atmospheric Infrared Sounder moisture accuracy, *J. Geophys. Res.*, *112*, D13S90, doi:10.1029/2005JD006109.

Miloshevich, L. M., H. Vömel, D. Whiteman, B. Lesht, F. J. Schmidlin, and F. Russo (2006), Absolute accuracy of water vapor measurements from six operational radiosonde types launched during AWEX-G and implications for AIRS validation, *J. Geophys. Res.*, *111*, D09S10, doi:10.1029/2005JD006083.

Minschwaner, K., and A. E. Dessler (2004), Water vapor feedback in the tropical upper troposphere: Model results and observations, *J. Clim.*, *17*, 1272–1281.

Nalli, N. R., et al. (2006), Ship-based measurements for infrared sensor validation during Aerosol and Ocean Science Expedition 2004, *J. Geophys. Res.*, *111*, D09S04, doi:10.1029/2005JD006385.

Pagano, T. S., H. H. Aumann, D. E. Hagan, and K. Overoye (2003), Prelaunch and in-flight radiometric calibration of the Atmospheric Infrared Sounder (AIRS), *IEEE Trans. Geosci. Remote Sens.*, *41*, 265–273.

Parkinson, C. L. (2003), Aqua: An earth-observing satellite mission to examine water and other climate variables, *IEEE Trans. Geosci. Remote Sens.*, *41*, 173–183.

Peter, T., C. Marcolli, P. Spichtinger, T. Corti, M. B. Baker, and T. Koop (2006), When dry air is too humid, *Science*, *314*, 1399–1402.

Read, W. G., et al. (2001), UARS MLS upper tropospheric humidity measurement: Method and validation, *J. Geophys. Res.*, *106*, 32,207–32,258.

Read, W. G., Z. Shippony, and W. V. Snyder (2006), The clear-sky unpolarized forward model for the EOS Aura microwave limb sounder (MLS), *IEEE Trans. Geosci. Remote Sens.*, *44*, 1367–1379.

Read, W. G., et al. (2007), Aura Microwave Limb Sounder upper tropospheric and lower stratospheric H_2O and relative humidity with respect to ice validation, *J. Geophys. Res.*, *112*, D24S35, doi:10.1029/2007JD008752.

Rodgers, C. D., and B. J. Connor (2003), Intercomparison of remote sounding instruments, *J. Geophys. Res.*, *108*(D3), 4116, doi:10.1029/2002JD002299.

Rossow, W. B., and R. A. Schiffer (1999), Advances in understanding clouds from ISCCP, *Bull. Am. Meteorol. Soc.*, *80*, 2261–2287.

Schoeberl, M. R., et al. (2006), Overview of the EOS Aura mission, *IEEE Trans. Geosci. Remote Sens.*, *44*(5), 1066–1074.

Sherwood, S. C., and A. E. Dessler (2001), A model for transport across the tropical tropopause, *J. Atmos. Sci.*, *58*, 765–779.

Soden, B. J. (2000), The diurnal cycle of convection, clouds, and water vapor in the tropical upper troposphere, *Geophys. Res. Lett.*, *27*, 2173–2176.

Soden, B. J., and F. P. Bretherton (1993), Upper-tropospheric relative-humidity from the GOES 6.7 um channel: Method and climatology for July 1987, *J. Geophys. Res.*, *98*, 16,669–16,688.

Soden, B. J., and I. M. Held (2006), An assessment of climate feedbacks in coupled atmosphere-ocean models, *J. Clim.*, *19*, 3360–3554.

Stephens, G. L. (2005), Cloud feedbacks in the climate system: A critical review, *J. Clim.*, *18*, 237–273.

Stephens, G. L., et al. (2002), The CloudSat Mission and the A-Train: A new dimension of space-based observations of clouds and precipitation, *Bull. Am. Meteorol. Soc.*, *83*, 1771–1790.

Strow, L. L., S. E. Hannon, S. De Souza-Machado, H. E. Motteler, and D. Tobin (2003), *IEEE Trans. Geosci. Remote Sens.*, *41*, 303–313.

Strow, L. L., S. E. Hannon, S. De-Souza Machado, H. E. Motteler, and D. C. Tobin (2006), Validation of the Atmospheric Infrared Sounder radiative transfer algorithm, *J. Geophys. Res.*, *111*, D09S06, doi:10.1029/2005JD006146.

Su, H., W. G. Read, J. H. Jiang, J. W. Waters, D. L. Wu, and E. J. Fetzer (2006a), Enhanced positive water vapor feedback associated with tropical deep convection: New evidence from Aura MLS, *Geophys. Res. Lett.*, *33*, L05709, doi:10.1029/2005GL025505.

Su, H., D. E. Waliser, J. Jiang, J. Li, W. G. Read, J. W. Waters, and A. Tompkins (2006b), Relationships of upper tropospheric water vapor, clouds and SST: MLS observations, ECMWF analyses and GCM simulations, *Geophys. Res. Lett.*, *33*, L22802, doi:10.1029/2006GL027582.

Susskind, J., C. D. Barnet, and J. M. Blaisdell (2003), Retrieval of atmospheric and surface parameters from AIRS/AMSU/HSB data in the presence of clouds, *IEEE Trans. Geosci. Remote Sens.*, *41*, 390–409.

Susskind, J., C. Barnet, J. Blaisdell, L. Iredell, F. Keita, L. Kouvaris, G. Molnar, and M. Chahine (2006), Accuracy of geophysical parameters derived from Atmospheric Infrared Sounder/Advanced Microwave Sounding Unit as a function of fractional cloud cover, *J. Geophys. Res.*, *111*, D09S17, doi:10.1029/2005JD006272.

Tian, B. J., B. J. Soden, and X. Q. Wu (2004), Diurnal cycle of convection, clouds, and water vapor in the tropical upper troposphere: Satellites versus a general circulation model, *J. Geophys. Res.*, *109*, D10101, doi:10.1029/2003JD004117.

Tian, B., D. E. Waliser, E. J. Fetzer, B. H. Lambrigtsen, Y. L. Yung, and B. Wang (2006), Vertical moist thermodynamic structure and spatial-temporal evolution of the Madden-Julian oscillation in Atmospheric Infrared Sounder observations, *J. Atmos. Sci.*, *63*, 2462–2485.

Tobin, D. C., H. E. Revercomb, R. O. Knuteson, B. Lesht, L. L. Strow, S. E. Hannon, W. F. Feltz, L. Moy, E. J. Fetzer, and T. Cress (2006), Atmospheric radiation measurement site atmospheric state best estimates for Atmospheric Infrared Sounder temperature and water vapor retrieval validation, *J. Geophys. Res.*, *111*, D09S14, doi:10.1029/2005JD006103.

Vömel, H., et al. (2007), Validation of Aura/MLS water vapor by balloon borne Cryogenic Frostpoint Hygrometer measurements, *J. Geophys. Res.*, *112*, D24S37, doi:10.1029/2007JD008698.

Waters, J. W., et al. (2006), The Earth Observing System Microwave Limb Sounder (EOS MLS) on the Aura satellite, *IEEE Trans. Geosci. Remote Sens.*, *44*(5), 1075–1092.

Whiteman, D., et al. (2006), Analysis of Raman lidar and radiosonde measurements from the AWEX-G field campaign and its relation to Aqua validation, *J. Geophys. Res.*, *111*, D09S09, doi:10.1029/2005JD006429.

Wilks, D. S. (2006), *Statistical Methods in the Atmospheric Science*, Academic, London, U.K.

World Meteorological Organization (1957), Definition of the tropopause, *WMO Bull.*, *6*, 136.

Wu, D. L., W. G. Read, A. E. Dessler, S. C. Sherwood, and J. H. Jiang (2005), UARS/MLS cloud ice measurements: Implications for H_2O transport near the tropopause, *J. Atmos. Sci.*, *62*, 518–530.

Wu, D. L., J. H. Jiang, and C. P. Davis (2006), EOS MLS cloud ice measurements and cloudy-sky radiative transfer model, *IEEE Trans. Geosci. Remote Sens.*, *44*(5), 1156–1165.

Yanai, M., S. Esbensen, and J. Chu (1973), Determination of bulk properties of tropical cloud clusters from large-scale heat and moisture budgets, *J. Atmos. Sci.*, *30*, 611–627.

Ye, H., E. J. Fetzer, D. H. Bromwich, E. F. Fishbein, E. T. Olsen, S. Granger, S.-Y. Lee, L. Chen, and H. Bjorn Lambrigtsen (2007), Atmospheric total precipitable water from AIRS and ECMWF during Antarctic summer, *Geophys. Res. Lett.*, *34*, L19701, doi:10.1029/2006GL028547.

V. Dang, M. de la Torre Juarez, A. Eldering, E. J. Fetzer, F. W. Irion, J. Jiang, B. H. Kahn, W. G. Read, H. Su, and D. Waliser, Jet Propulsion Laboratory, California Institute of Technology, MS 169-237, 4800 Oak Grove Drive, Pasadena, CA 91109, USA. (eric.j.fetzer@jpl.nasa.gov)

B. Tian, Jet Propulsion Laboratory, California Institute of Technology, 4800 Oak Grove Drive, Pasadena, CA 91109, USA.

H. Vömel, Deutscher Wetterdienst, Am Observatorium 12, 15848 Tauche/Lindenberg, Germany.